

Dynamic visco-hyperelastic behavior of elastomeric hollow cylinder by developing a constitutive equation

Masoud Asgari* and Sanaz S. Hashemi^a

Faculty of Mechanical Engineering, K. N. Toosi University of Technology, Tehran, Iran

(Received December 7, 2015, Revised April 6, 2016, Accepted April 15, 2016)

Abstract. In this study, developments of an efficient visco-hyperelastic constitutive equation for describing the time dependent material behavior accurately in dynamic and impact loading and finding related materials constants are considered. Based on proposed constitutive model, behaviour of a hollow cylinder elastomer bushing under different dynamic and impact loading conditions is studied. By implementing the developed visco-hyperelastic constitutive equation to LS-DYNA explicit dynamic finite element software a three dimensional model of the bushing is developed and dynamic behaviour of that in axial and torsional dynamic deformation modes are studied. Dynamic response and induced stress under different impact loadings which is rarely studied in previous researches have been also investigated. Effects of hyperelastic and visco-hyperelastic parameters on deformation and induced stresses as well as strain rate are considered.

Keywords: visco-hyperelastic constitutive equation; elastomer bushing; impact loading; explicit FEM

1. Introduction

The natural rubber was firstly made of a kind of latex material from a special plant in 1600 BC by Mayans for making playing balls Martinez (2006). Since then, elastomers have had a various application such as industry and military Okwu and Okieimen (2011). Nowadays large variety of elastomers are produced having wide and ever increasing applications in several industries such as shock absorbers, bridge and building bearings and automotive industry where rubbers are used as mechanical sealing, mountings, gaskets, components of suspension system and etc., Gent (1996).

On the other hand by developing of complicated non-linear materials such as rubbers, appropriate modelling of these materials have been became one of the crucial issues in industries and research studies. The mechanical behaviour of the elastomers is dominated by nonlinear rate-dependent response (Amin *et al.* 2002). Hence, to reproduce the general mechanical behaviour of these materials, it is necessity to develop a constitutive model that can simulate the rate-dependent nonlinear characteristics. Comprehensive investigations have been made to study and model the elastomers static and time dependent behaviour (Yeoh and Fleming 1997, Bechir 2006, Aniskevich *et al.* 2010, Diani *et al.* 2006, Holzapfel 1996, Kim *et. al* 2014, Luis 2015). These models are

*Corresponding author, Assistant Professor, E-mail: asgari@kntu.ac.ir

^aM.Sc. Student, E-mail: saadatmand@kntu.ac.ir

mainly including two categories of equilibrium and time-dependent models. The early work was related to the predictions of the equilibrium response Ouyang (2006). While, there exist fewer models that consider the time dependence for finite strain deformations James and Guth (1943). Bergstrom and Boyce (1998) studied the nonlinear time-dependence deviation from the equilibrium state by use of a spring-dashpot network. (Yang *et al.* 2002, 2004) developed a visco-hyperelastic model for rubber under high strain rate considers the three-dimensional large compression behavior of rubbers at the different strain rates using BKZ theory. Some three-parameter models including multiplicative decompositions of deformation tensor and application of second thermodynamic law introduced by Huber and Tsakmakis (2000). (Admin *et al.* 2002) captured the rate-dependent behavior of natural and high damping natural rubbers based on the models proposed by Huber and Tsakmakis (2000).

Elastomer bushings are one of those critical components in some mechanical systems especially in vehicle suspension systems exerted large and time varying loads and deformations. Most of the bushings are composed of a hollow elastomer cylinder contained between inner and outer cylindrical steel sleeves. The most usual deformation modes about elastomeric bushings are torsional and axial modes (Kadlowec *et al.* 2009). It is clear that appropriate material model selection and determination of its parameters effect on the accuracy of results of the finite element analysis of rubber components such as rubber bearings and elastomer bushings. The main material models used for bushings are hyper-elastic constitutive equations in which the time and rate dependency of behaviour should be neglected. Adkins and Gent (1954) theoretically and experimentally investigated force-deformation relations for small deformations of bonded rubber bushings. The stiffness of rubber bush mountings was studied by (Horton *et al.* 2000, Busfield and Davies 2001). Chen and Wu (1997) studied computational issues associated with nonlinear bushing analysis, comparing the results using two different material models with experimental data from tension-compression and shear tests. Kadlowec (2001, 2003) conducted experiments and modeled coupled radial- torsional deformation modes of elastomer bushing.

For analyses containing time and rate dependency such as cyclic loading or dynamic impact analysis, hyper elastic models does not provide enough accuracy and so viscoelastic effects also must be included in the material model. It leads to a new generation of constitutive equations called visco-hyperelastic.

Naghdabadi *et al.* (2012) proposed a constitutive model based on the logarithmic strain to analyze the behavior of elastomeric bushings in torsional and radial deformations. (Kadlowec *et al.* 2009) conducted an experimental study on the behavior of the elastomeric bushings in torsional and combined torsional-axial modes. (Khajehsaeid *et al.* 2013) also considered numerical analysis of Finite strain of elastomeric bushings under multi-axial loadings proposing a compressible visco-hyperelastic approach. (Karimi *et al.* 2014) presented a visco-hyperelastic constitutive approach for modeling polyvinyl alcohol sponge. They propose the quasi-linear viscoelastic (QLV) model to characterize the time dependent mechanical behavior of poly (vinyl alcohol) (PVA) sponges. The PVA sponges have implications in many viscoelastic soft tissues, including cartilage, liver, and kidney as an implant. However, a critical barrier to the use of the PVA sponge as tissue replacement material is a lack of sufficient study on its viscoelastic mechanical properties. They investigate the nonlinear mechanical behavior of a fabricated PVA sponge experimentally and computationally using relaxation and stress failure tests as well as finite element (FE) modeling. Hyperelastic strain energy density functions, such as Yeoh and Neo-Hookean, are used to capture the mechanical behavior of PVA sponge at ramp part, and viscoelastic model is used to describe the viscose behavior at hold part. Wang *et al.* (2015) presented a general visco-hyperelastic model

for dielectric elastomers (DE) which derived from the Quasi-Linear Viscoelastic (QLV) framework. To gain a physical insight into the time-dependent constitutive relation and solve it efficiently, they specifically constructed a complex frequency representation of the convolution integral equation, with the legible form of block-scheme, in which the viscoelastic stress is interpreted considering the instantaneous response (depicted by Yeoh strain energy potential) as a signal filtered by a linear system (superposition of characteristic modes of the time relaxation function, i.e., Prony series).

(Rodas *et al.* 2016) presented a thermo-visco-hyperelastic model for the heat build-up during low-cycle fatigue of filled rubbers: Formulation, implementation and experimental verification. They have been developed a finite strain thermo-visco-elastic constitutive model, in accordance with the second thermodynamics principle to predict the heat build-up field in rubbers during low-cycle fatigue.

As it is clear in previous studies the main concerns were on quasi static deformation and simple standard tests of elastomer bushings. While the main loadings experienced by these element are impact and severe dynamics one. Few researches seen on shock loadings have not considered viscoelastic effects Niles and Adivi (2011), Hakansson (2000). To this end investigation of elastomer bushings behaviour under impact loading considering visco-hyper-elastic effects could be of great importance.

In this study, some well-known strain energy functions including Neo-Hookean, Mooney-Rivlin and Ogden calibrated by experimental data of the specified elastomer have been used to find precisely constitutive equation and related material constants for large deformation behaviour. By choosing the best hyperelastic model and determining its parameters a nonlinear visco-hyperelastic constitutive equation has been developed and calibrated based on some existing experimental data in order to contain time and strain rate dependency of the material. Material parameters are determined using an efficient optimization algorithm for both models. By implementing the developed visco-hyperelastic constitutive equation to LS-DYNA explicit dynamic finite element software a three dimensional model of the bushing is developed and dynamic behaviour of that in axial and torsional deformation modes are considered. On the other hand because of common impact loading of the bushings, dynamic response and induced stress under different impact loads have been modelled. The effect of viscoelastic characteristics coupled with hyperelastic behaviour are studied through this way. According to the obtained results, although hyperelastic models describe elastomers' behavior but by considering time dependency in these materials, it could be seen that developed visco-hyperelastic model describes these materials more accurately. On the other hand deformation and induced stresses differ considerably by changing the loading rate. It can be concluded that considering viscos effects and time dependency by using visco-hyperelastic model leads us to more accurate results. Comparing two types of impact loading indicates that the transversal loading is more destructive.

2. Material modelling

2.1 Hyperelastic material modelling

Large extension feature of rubbery materials motivated researchers over decades to express the associated nonlinear elastic behavior through hyperelastic models (Amin *et al.* 2002). Hyperelastic or Green elastic material is a type of constitutive model for ideally elastic material for which the

stress-strain relationship derives from a strain energy density function Niles and Adivi (2009). For rubber like materials, linear elastic models do not accurately describe the observed material behaviour in large strain response regime. Hyperelasticity provides a means of modelling the stress-strain behavior of such materials. The strain energy density W is a scalar function of one tensorial variable, i.e., the deformation gradient \mathbf{F} . For isotropic elastic materials, the strain energy function W can be expressed as a function of invariants of a deformation tensor. For hyperelastic materials the strain energy density function is defined in a general way as

$$W(E_{ij}) = \int_0^{E_{ij}} S_{ij}(E_{ij}) dE_{ij} \quad (1)$$

Where E is the Green-Lagrange strain tensor and S is the second Piola-Kirchoffs stress tensor. Differentiation of the strain energy W with respect to the Lagrangian strain gives the energy conjugate second Piola-Kirchoff stress as

$$S = 2 \frac{\partial W}{\partial C} \quad (2)$$

Where C is the Right Cauchy-Green strain tensor defined as

$$E = \frac{(C - I)}{2} \quad (3)$$

For isotropic elastic materials, the strain energy function W can be expressed as a function of invariants of a deformation tensor as Holzapfel (1996)

$$W = W[I_1(C), I_2(C), I_3(C)] \quad (4)$$

The three strain invariants of the Right Cauchy-Green strain tensor can be expressed as

$$\begin{aligned} I_1 &= \text{tr}C = \lambda_1^2 + \lambda_2^2 + \lambda_3^2 \\ I_2 &= \frac{1}{2}[(\text{tr}C)^2 - \text{tr}(C^2)] = \lambda_1^2 \lambda_2^2 + \lambda_1^2 \lambda_3^2 + \lambda_2^2 \lambda_3^2 \\ I_3 &= J^2 = \lambda_1^2 \lambda_2^2 \lambda_3^2 \end{aligned} \quad (5)$$

By expanding the Eq. (2) we have

$$\frac{\partial W(C)}{\partial C} = \frac{\partial W}{\partial I_1} \frac{\partial I_1}{\partial C} + \frac{\partial W}{\partial I_2} \frac{\partial I_2}{\partial C} + \frac{\partial W}{\partial I_3} \frac{\partial I_3}{\partial C} \quad (6)$$

Where the components of Eq. (6) can be derived as follow

$$\frac{\partial I_1}{\partial C_{ij}} = \delta_{ij}, \frac{\partial I_2}{\partial C_{ij}} = I_1 \delta_{ij} - C_{ij}, \frac{\partial I_3}{\partial C_{ij}} = I_3 C_{ij}^{-1} \quad (7)$$

Finally according to Eqs. (2), (6) and (7) we derive second Piola-Kirchoffs stress tensor

$$S = 2 \left[\left(\frac{\partial W}{\partial I_1} + I_1 \frac{\partial W}{\partial I_2} \right) I - \frac{\partial W}{\partial I_2} C + I_3 \frac{\partial W}{\partial I_3} C^{-1} \right] \quad (8)$$

The relation of second Piola-Kirchoffs stress tensor and Cauchy stress tensor can be define as

Holzappel (1996)

$$\sigma = J^{-1}FSF^T \tag{9}$$

By substituting Eq. (8) in Eq. (9) we derive the general form of Cauchy stress as

$$\sigma = 2J^{-1} \left[\left(\frac{\partial W}{\partial I_1} + I_1 \frac{\partial W}{\partial I_2} \right) B - \frac{\partial W}{\partial I_2} B^2 + I_3 \frac{\partial W}{\partial I_3} I \right] \tag{10}$$

Where B is the Left Cauchy-Green strain tensor. To determine the hyperelastic model for the elastomer bushing the potential functions will be considered are Ogden, Neo-Hookean and Mooney-Rivlin (Ogden 1972, Rivlin and Barenblatt 1997, Macosko and Larson 1994) in the following sections.

2.2 Viscoelastic material modelling

Viscoelastic materials, like rubbers, resist shear flow and when a stress is applied they strain linearly with time and also strain when stretched and quickly return to their original state once the stress is removed. Whereas elasticity is usually the result of bond stretching along crystallographic planes in an ordered solid, viscosity is the result of the diffusion of atoms or molecules inside an amorphous material Hakansson (2007). In order to conclude the strain-rate dependency of elastomers, the proposed hyperelasticity relation will be employed to describe the equilibrium and instantaneous state boundaries that exist in the responses of any typical viscoelastic solid.

The viscoelastic behaviour can be divided into large and small deformation. Where the strain is small just initial values of shear and Bulk modulus would be enough as the starting values of the material properties through the time. These shear and bulk modules are representative of deviatoric and volumetric parts of the stress respectively

$$\sigma = \sigma_{\text{deviatoric}} + \sigma_{\text{volumetric}} \tag{11}$$

and then we have

$$\sigma = \int_0^t 2g(t-\tau) \frac{de}{d\tau} d\tau + I \int_0^t k(t-\tau) \frac{d\Delta}{d\tau} d\tau \tag{12}$$

Where σ is Cauchy stress, e and Δ are deviatoric and volumetric part of the strains. $g(t)$ and $k(t)$ are shear and Bulk modulus functions, t and τ are current and past time and I is identity matrix. Shear and bulk modulus are related over the time by Prony series equations as Björnsson and Danielsson (1995)

$$g(t) = g_0 \left[g_\infty + \sum_{i=1}^n g_i \exp\left(-\frac{t}{\tau_i}\right) \right] \tag{13}$$

$$k(t) = k_0 \left[k_\infty + \sum_{i=1}^n k_i \exp\left(-\frac{t}{\tau_i}\right) \right] \tag{14}$$

$g_i = G_i/G_0$ and τ_i is relaxation time constant for each Prony series component. g_∞ could be simply calculated by setting t equal to zero. Then Eq. (13) changes as

$$G_0 = G_0 \left[g_\infty^G + \sum_{i=1}^{n_G} g_i^G \right] \quad (15)$$

Where the term $\left[g_\infty^G + \sum_{i=1}^{n_G} g_i^G \right]$ should then be equal to 1. It means that $g_\infty^G = 1 - \sum_{i=1}^{n_G} g_i^G$.

Hence, the only constants of the formula are g_i and τ_i which should be determined by a relaxation test. By choosing the number of Prony components and performing a curve fitting coming from the experimental results of relaxation test, we can get the unknown coefficients and model our viscoelastic material based on Prony series.

2.3 Visco-hyperelastic constitutive equation

Hyperelastic model are used to represent the response of elastomer at a particular strain rate assuming complete elastic recovery of the material. However, in order to model the rate dependency, the hyperelastic models are required to be combined with a rate-dependent model to represent the equilibrium and instantaneous responses. To this end, this section proposes a hyperelastic model and its incorporation into a rate-dependent model structure to derive the final model. A simple model for computing the strain and the time dependent constants for non-linear Visco-hyperelastic materials is presented. A common method for determining the large strain viscoelastic behaviour is based on the finite time increment formulation of the convolution integral, and is applicable for materials which exhibit separable strain and time variables.

The strain-dependent function can take any form including the hyperelastic potentials strain energy function. The time-dependent function is based on the Prony series.

Thus, in non-linear visco-hyperelasticity the stress depends on both time and strain. Then general constitutive equation can be formulated in the form of convolution of the strain-dependent part which here can take any form of hyperelastic models and the time-dependent part which is a function based on prony series. Generally, the stress function of a visco-hyperelastic material is given in an integral form. The second Piola-Kirchhoff stress tensor (S_{ij}) can be written as Fung (1965)

$$S(\lambda, t) = \sigma^e(\lambda) * g(t) \quad (16)$$

Where $\sigma^e(\lambda)$ is strain-dependant function and $g(t)$ time dependant function. The sign * denotes the convolution of σ_e and g . The function $g(t)$ may be defined by means of the Prony series explained in Eq. (13) Using convolution integral of S and g , the equation takes the form of

$$S(\lambda, t) = \int_0^t g(t-s) \frac{\partial S^e(\lambda)}{\partial \lambda} \frac{\partial \lambda}{\partial s} ds \quad (17)$$

Assuming that the relaxation function is the same in all directions, the stress relaxation tensor becomes a scalar, and referring to the work of Simo and Holzapfel (1996), the visco-hyperelastic constitutive equations of the second Piola-Kirchhoff stress is given as

$$S(t) = g_\infty \sigma^e(t) + \sum_{i=1}^n \int_0^t g_i \exp\left(-\frac{t-s}{\tau_i}\right) \frac{\partial \sigma^e(s)}{\partial s} ds \quad (18)$$

The stress $S(\lambda, t)$ in Eq. (17) is now a function of only time t if the strain history $\lambda(t)$ is known. The integral in Eq. (18) may be computed using the algorithm presented in Goh *et al.* (2004),

which is based on finite increments of time. Following the derivation introduced in Goh *et al.* (2004), Eq. (15) can be written in the form of

$$S(t+1) = g_{\infty} \sigma^e(t+1) + \left[\sum_{i=1}^n \exp\left(-\frac{\Delta t}{\tau_i}\right) h_i(t) + g_i \frac{\left(1 - \exp\left(-\frac{\Delta t}{\tau_i}\right)\right)}{\frac{\Delta t}{\tau_i}} (\sigma^e(t+1) - \sigma^e(t)) \right] \quad (19)$$

Where Δt is the time increment. As the initial stress and strain in the material are known, the stress at time $t > 0$ can be easily calculated.

3. Parameter optimization for constitutive equations

3.1 Parameter optimization for the hyperelastic constitutive equations

Determining of the materials parameters require experimental tests. Firstly an analytical solutions of the equations is derived in uniaxial tests for some well-known strain energy models. By deriving the Cauchy stress function for different models by the methods aforementioned before, the material parameters can be determined by substituting experimental tensile test data into each of models using the Levenberg-Marquardt Moré (1967) nonlinear curve fitting algorithm. The strain energy function for Neo-Hookean model is

$$W = C_{10} (I_B - 3) \quad (20)$$

So by substituting Eq. (20) in Eq. (10) the Cauchy stress can be readily derived as

$$\sigma = 2C_{10} \left(\lambda^2 - \frac{1}{\lambda} \right) \quad (21)$$

3.1.1 Levenberg least square optimization method

The Levenberg-Marquardt method is a standard technique used to solve nonlinear least squares problems. Least squares problems arise when fitting a parameterized function to a set of measured data points by minimizing the sum of the squares of the errors between the data points and the function. Nonlinear least squares problems arise when the function is not linear in the parameters. Nonlinear least squares methods involve an iterative improvement to parameter values in order to reduce the sum of the squares of the errors between the function and the measured data points (Moré 1978). The Levenberg-Marquardt curve-fitting method is actually a combination of two minimization methods: the gradient descent method and the Gauss-Newton method. In the gradient descent method, the sum of the squared errors is reduced by updating the parameters in the steepest-descent direction. In the Gauss-Newton method, the sum of the squared errors is reduced by assuming the least squares function is locally quadratic, and finding the minimum of the quadratic. The Levenberg-Marquardt method acts more like a gradient-descent method when the parameters are far from their optimal value, and act more like the Gauss-Newton method when the parameters are close to their optimal value. Here we write the standard form of the

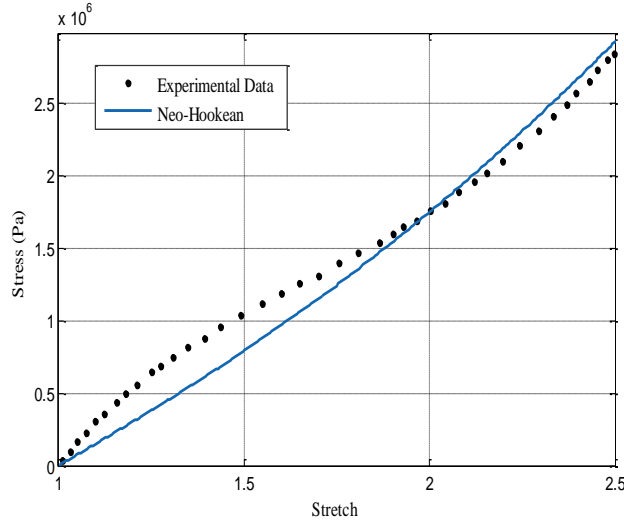


Fig. 1 Curve fitting of experimental data using Neo-Hookean models

optimization problem aforementioned above as we said the cost function will be form as below (Gavin 2011)

$$\min f(\lambda) = \min \sum_{i=1}^n R_i^2(\lambda) \tag{22}$$

Where each R_i is called residual that determined as follow

$$R_i(\lambda) = \sigma(\lambda_i) - \sigma_i \tag{23}$$

Where σ_i are the experimental data's at each λ_i .

The algorithm for Levenberg-Marquardt is as follow:

1. First estimate $X_0, k=0, select \ \varepsilon=1, \beta_0=1$
2. Calculate $C^k = \frac{\partial f(x^k)}{\partial x}$ if $\|C^k\| \leq \varepsilon \rightarrow stop$
3. Search direction $d^k = -[H^k + \beta_k I]^{-1} C^k$ where H is the hessian and I identity matrix.
4. if $f(x^k + d^k) \leq f(x^k)$ then reduce β_k

By using the aforementioned algorithm we fitted curve on experimental data provided by Kadlowec *et al.* (2003) for Neo-Hookean model as shown in Fig. 1.

The related constant is obtained as $C_{10}=1.071e+0.5$.

Using the *two* terms Mooney-Rivlin model and its derived stress as

$$\begin{aligned} W &= C_{10}(I_1 - 3) + C_{01}(I_2 - 3) \\ \sigma &= 2\left(C_{10} + C_{01}\frac{1}{\lambda}\right)\left(\lambda^2 - \frac{1}{\lambda}\right) \end{aligned} \tag{24}$$

The best fitted curve by Levenberg algorithm demonstrated in Fig. 2 and its parameters defined as $C_{10}=1.071e^{+5}$ and $C_{01}=3.111e^{+5}$.

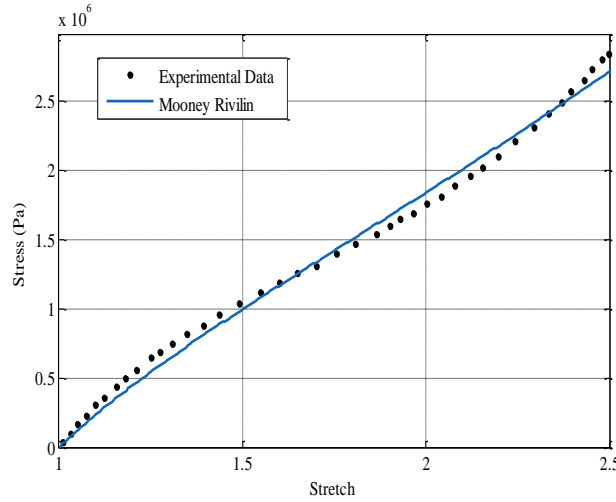


Fig. 2 Curve fitting of experimental data using Mooney-Rivlin models

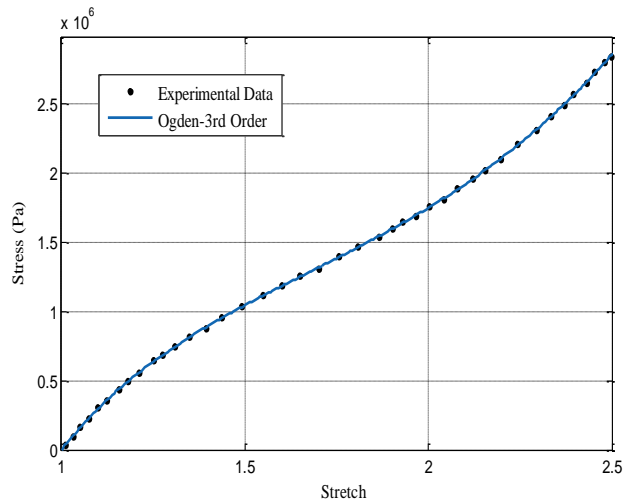


Fig. 3 Curve fitting of experimental data using 3rd Ogden model

Finally the strain energy function for the Ogden model is presented as

$$W = \sum_{n=1}^N \frac{\mu_n}{\alpha_n} (\lambda_1^{\alpha_n} + \lambda_2^{\alpha_n} + \lambda_3^{\alpha_n} - 3) \tag{25}$$

Combining Eqs. (2)-(10) and Eqs. (3)-(4) the Cauchy stress tensor for Ogden model derived as following

$$\sigma = \frac{2}{\lambda^2} \left\{ \frac{\mu_1}{\alpha_1} \left(\lambda^{\alpha_1} - \lambda^{-\frac{\alpha_1}{2}} \right) + \frac{\mu_2}{\alpha_2} \left(\lambda^{\alpha_2} - \lambda^{-\frac{\alpha_2}{2}} \right) + \frac{\mu_3}{\alpha_3} \left(\lambda^{\alpha_3} - \lambda^{-\frac{\alpha_3}{2}} \right) \right\} \tag{26}$$

The related best fitted curve on experimental data has been shown in Fig. 3.

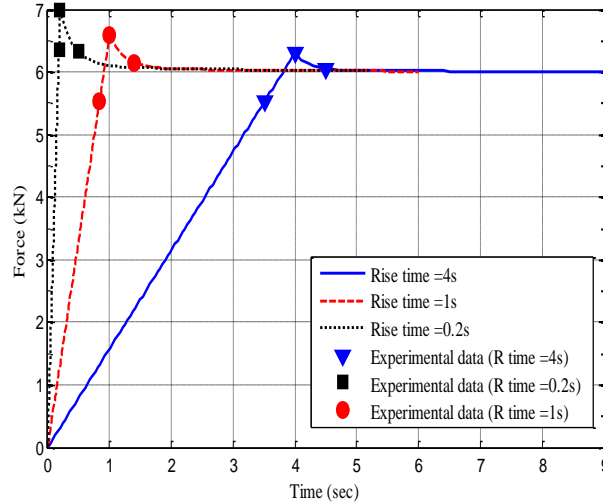


Fig. 4 relaxation responses of bushing under 1mm ramp axial displacement at rise times of 0.2, 1 and 4 sec

Then the best constants are derived as

$$\alpha_1 = 5.75, \alpha_2 = 0.5045, \alpha_3 = 0.5052, \mu_1 = 1.946e+04, \mu_2 = 1.825e+06, \mu_3 = 2.406e+06$$

By comparing Figs. 1-3, it is clearly seen that the Ogden material model appears to be best capture the bushing response. Then using this model for describing hyperelastic materials lead us to accurate results because of that in this paper we've used this model for predicting hyperelastic and visco-hyperelastic behavior of materials.

3.2 Parameter optimization for visco-hyperelastic constitutive equation

Based on the visco-hyperelastic constitutive equation derived in Eq. (19), the corresponding Prony series and Ogden models could be implemented in order to perform curve fitting on experimental data. There are unknown parameters from the Prony series model. For seeking the optimal parameters of the visco-hyperelastic model, an optimization scheme has been developed by using the Levenberg-Marquardt algorithm aforementioned above. Eq. (19) can be readily fitted to experimental stress-strain data which are measured at known time intervals to determine the material characteristics. The constant identification was performed by minimization of the error between the theoretical and experimental data in specified sampling time points. The optimization objective function is defined as

$$\min f(p) = \min \left(\sum_{i=1}^n \left[(S(t, p))_i - (S(t))_i \right]^2 \right) \quad (27)$$

The constraints defined in Eq. (27) have to be fulfilled by following conditions

$$0 \leq g_i < 1, \quad \sum_{i=1}^n g_i < 1, \quad \tau_i \geq 0 \quad (28)$$

Where $(S(t))_i$ are the values of stress measured at sampling times t_i , $i=1, \dots, l$, and $(S(t,p))_i$ are values of stress predicted by Eq. (18). The latter depends not only on time but also on the material parameters assembled in vector \mathbf{P} that exhibits as $\mathbf{P} = \{\alpha_1, \alpha_2, \alpha_3, \mu_1, \mu_2, \mu_3, g_1, g_2, g_3, \tau_1, \tau_2, \tau_3\}$. It should be noted that μ_i, α_i are the constants of Ogden model that has obtained at last part.

Validity of the proposed time-discrete form of the proposed visco-hyperelastic model has been examined by applying to the axial loading problem of a solid circular cylinder. Fig. 4 Illustrates force relaxation responses for ramp to 1mm axial displacement at rise times of 0.2, 1 and 4 sec. Solid lines results of the present work and symbols are experimental data Kadlowec (2009). Good agreement of results could be clearly seen.

Finally the unknown constants of visco-hyperelastic constitutive equation in vector \mathbf{p} determined as follow

$$g_i = (0.07, 0.02, 0.01)$$

$$\tau_i = (0.2, 0.3, 3)$$

4. Numerical results

To investigate performance of the constitutive model in three-dimensional boundary value problems, it is necessary to implement the model in finite element software. In this part, a hollow elastomer cylinder has been modelled in LS-DYNA explicit dynamic software and different loading scenarios including axial and torsional dynamic displacement modes and axial and lateral mode of impact have been considered. The developed visco-hyperelastic constitutive equation has been implemented in LS-DYNA. For describing the materials behaviour, we have compared both hyperelastic and visco-hyperelastic material models.

Elastomer bushing model is a variation of a production mold bonded bushing used in automotive suspension systems, and are of the type previously used by (Kadlowec *et al.* 2003). The bushings are manufactured by injection molding of the elastomeric material between inner and outer metal sleeves. The dimensions of the elastomer are 60 mm length, 18.2 mm outer radius and 9.85 mm inner radius shown in Fig. 5 which are the standard dimensions of elastomer bushings at industry (Hopkinton, Simple Bushings).

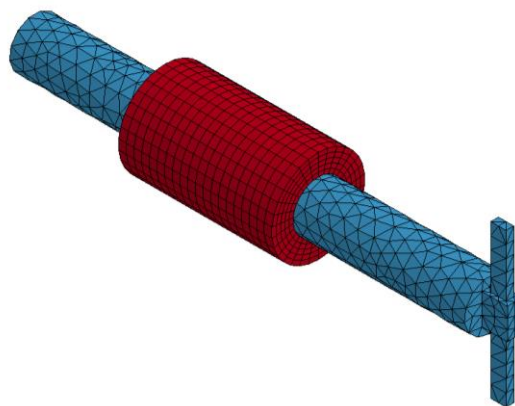


Fig. 5 Schematic of bushing sample including the loading rod

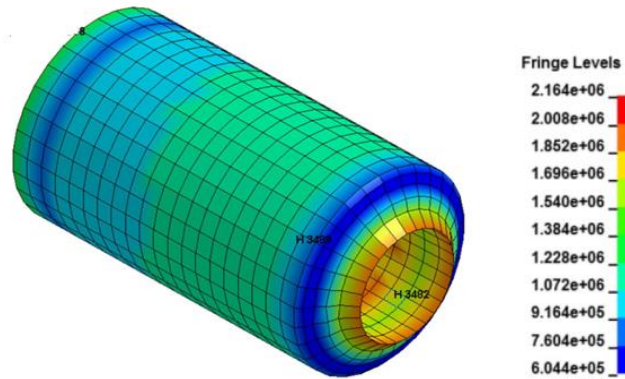


Fig. 6 Effective stress contour of bushing under axial displacement for load rating of 0.01

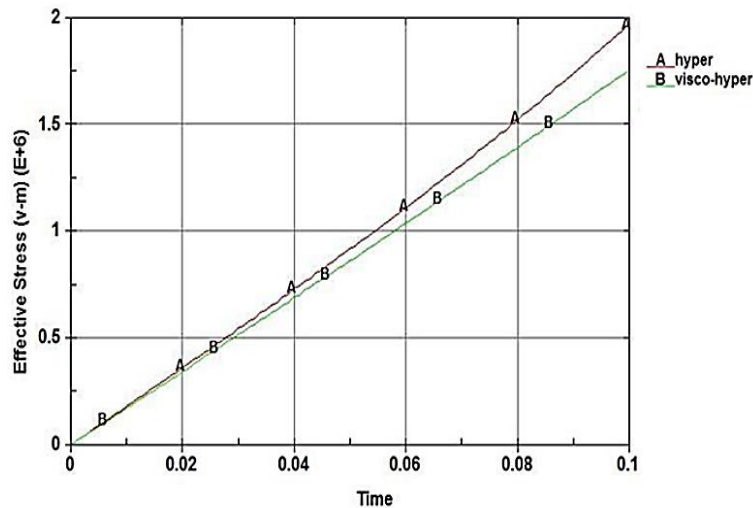


Fig. 7 Effective stress time history of axial mode for load rating of 0.01

To get accurate results, a mesh convergence analysis on a tubular structure with various different mesh sizes has been done. Element of different sizes are used to represent finer, fine, medium and coarse mesh effects and the mesh size of less than 2 mm produced acceptable results.

Automatic Surface to Surface” algorithm is used to model the contact between rigid impactor and rod in impact analysis. To avoid the zero energy deformation modes “Standard LS_DYNA viscous form” hourglass with coefficient of 0.1 was invoked.

4.1 Axial and torsional deformation modes

One-dimensional axial or torsional deformation modes were performed on the bushing conducted by holding the outer surface fixed and displacing the inner surface relative to the outer one. The main concern in this study is maximum effective stress created in the bushing and role of viscoelastic characteristics on that as well as time history of stresses. Distribution of effective stress shown in Fig. 6.

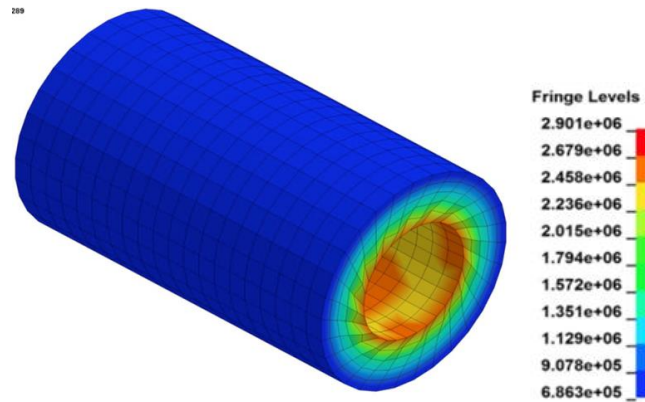


Fig. 8 Effective stress contour of bushing under torsional displacement for load rating of 0.01

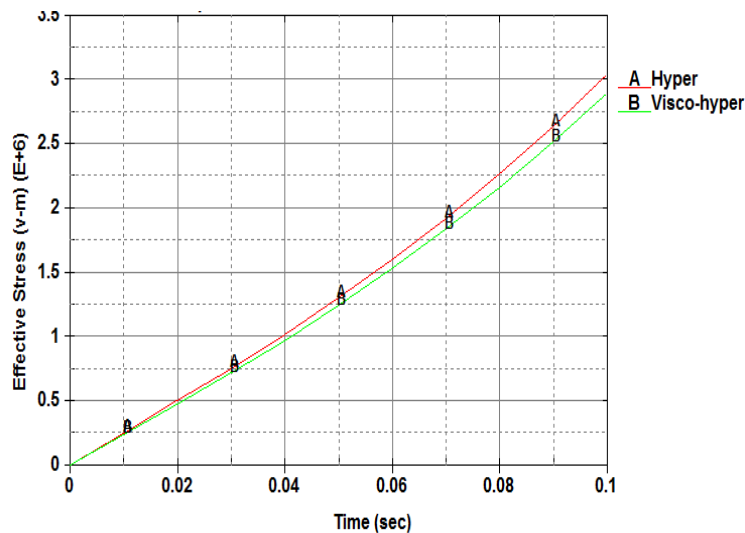


Fig. 9 Effective stress time history of torsional mode for load rating of 0.01

The time histories of effective stress concluding hyper elastic and visco-hyper elastic constitutive material models for a typical strain rate are also shown in Fig. 7. Difference of stress magnitude can be clearly seen in this figure. As it's clear we can see that at each time the magnitude of effective stress in hyper elastic model is greater than visco-hyper elastic model.

The same analysis has been also done for torsional deformation mode. A ramp to constant rotation was imposed on the inner bushing surface with a specified rate. The created effective stress is recorded for both the hyperelastic and visco-hyperelastic models. Fig. 8 shows stress distribution for a strain rate of 0.01.

A time history for these two constitutive equations is illustrated in Fig. 9. As we expect in this mode visco-hyper elastic model gives us again smaller effective stress than hyper elastic constitutive model.

For investigation of mechanical behaviour of the bushing in visco-hyperelastic regime, in which the relationship between stress and strain is not constant but rate-dependent, stress-strain

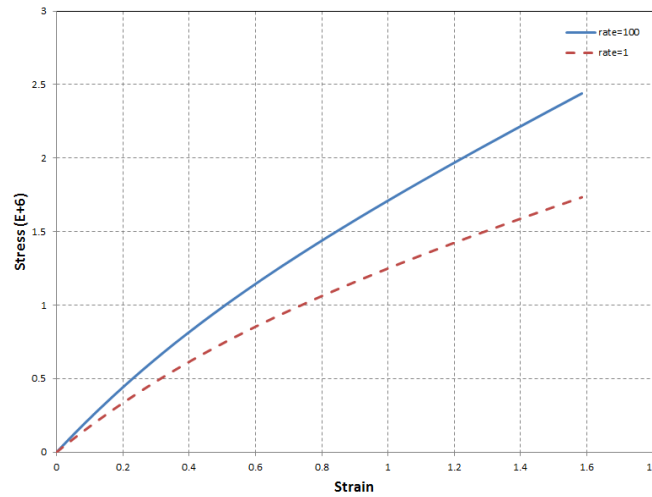


Fig. 10 Stress-Strain diagram at different rating for torsional mode

Table 1 Impact properties Centeno (2009)

Num. of test	Initial velocity $\frac{mm}{ms}$	Mass of impact(kg)
09615701	9.905	40.85

curve for the different strain rate has been illustrated in Fig. 10. It is clear that created stress is significantly greater in the bushing model under higher strain rate.

4.2 Impact loading

Most of the elastomer bushings placed in automotive exposed to different impacts during their life. Because of that in this part we've exposed the modelled hollow cylinder under different impact loadings. Using the calculated parameters for the visco-hyperelastic and hyperelastic models, we consider response of the bushing in the different impacts and investigate the effects of viscoelastic characteristics. The impact mass and velocity is defined based on impact test reference number 09615701 (Centeno 2009) as Table 1.

4.2.1 Axial impact

In this part we simulated an axial impact using LS-DYNA explicit finite element software as presented in Fig. 11. The Ogden strain energy used for hyperelastic model, while the proposed nonlinear visco-hyperelastic constitutive equation produced by combination of Ogden strain energy and Prony series visco elastic model implemented via LS-DYNA explicit dynamic solver in order to investigation of time dependent behaviour of material.

Fig. 12 Shows the time histories of effective stress for axial impact. The figure shows time dependent behaviour of the bushing affected by viscoelastic part of constitutive material modelling. The Maximum principal stress time history of a middle point of bushing under axial impact is also shown in Fig. 13. It can be clearly seen that peak stress for hyperelastic model is predicted considerably greater than visco-hyperelastic one.

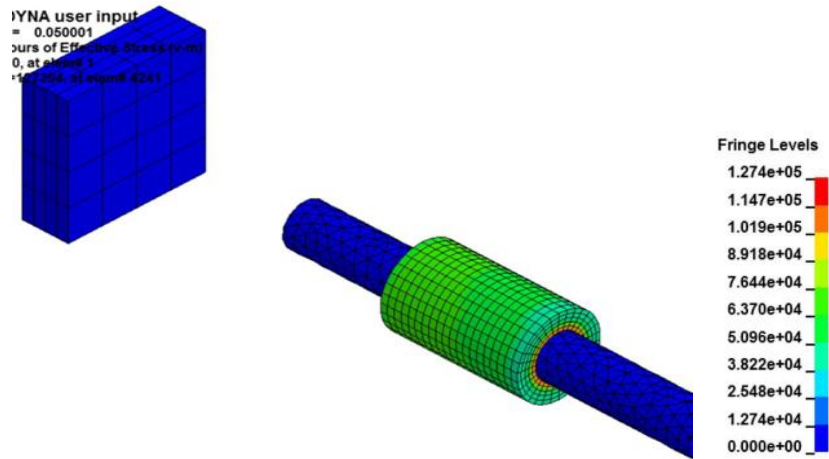


Fig. 11 Effective stress contour under axial impact at $t=0.05$ sec

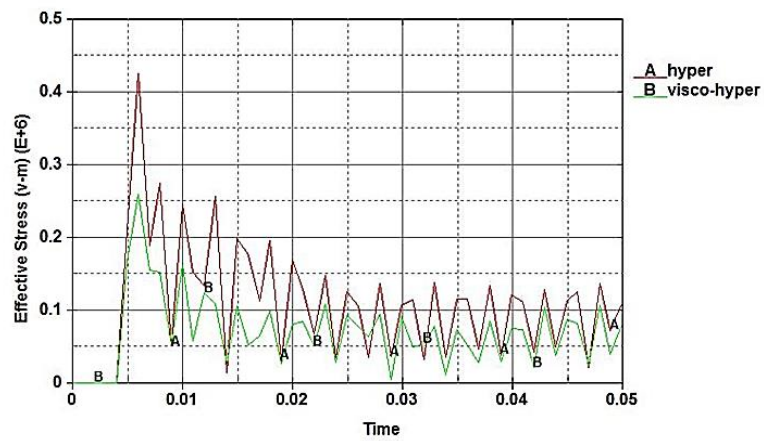


Fig. 12 Effective stress time history of a middle point of bushing under axial impact

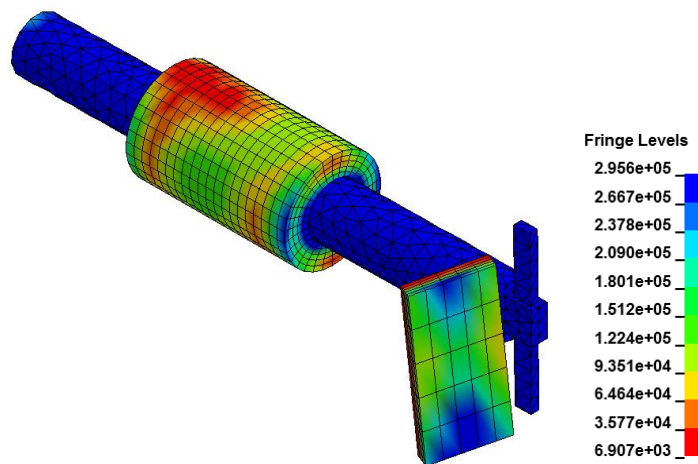


Fig. 13 Effective stress contour under transversal impact at $t=0.05$ sec

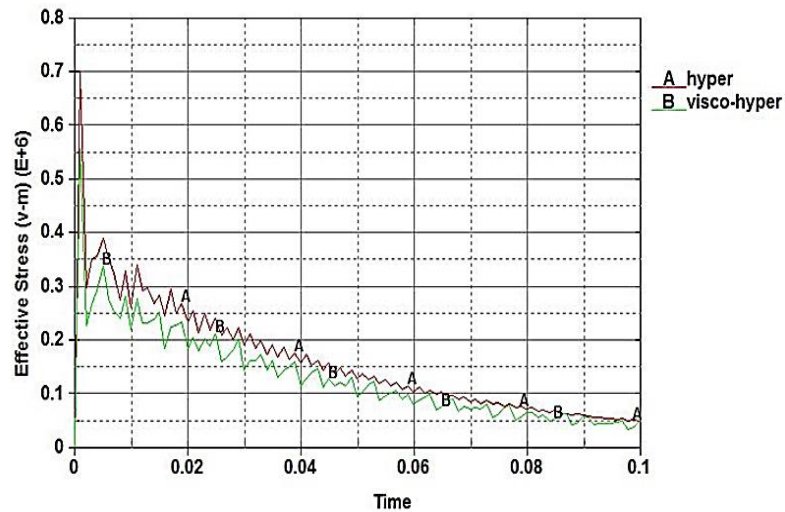


Fig. 14 The diagram of effective tension versus time under axial impact

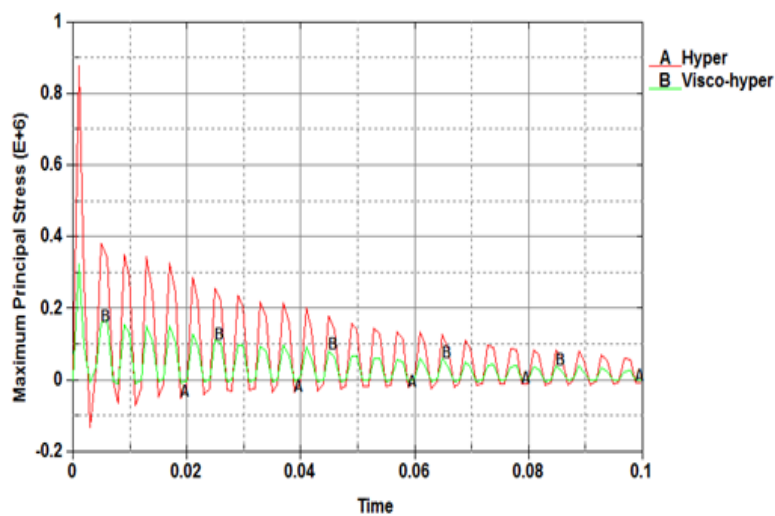


Fig. 15 Maximum principal stress time history of a middle point of bushing under transversal impact

4.2.2 Transverse impacts

The same analysis has been done for lateral impact as shown in Fig. 14.

Time history of effective stress related to lateral impact is shown in Fig. 15, in which the A line denotes the simulated results without considering the viscous part, and the B line represents the simulated results considering the viscous part. It can be seen that the maximum difference between these two curves is more than 21 percent, implying that the effect of the viscous part on the hyperelastic property of the bushing is apparent. Fig. 16 illustrates the Maximum principal stress time history of a middle point of bushing under transversal impact. The difference between two models is clearly seen here.

A comparison between the obtained results shows that the conventional hyperelastic strain energy functions could not be used to accurately describe these dynamic stress variations. The peak value as well as time history is different significantly regarded to visco-hyperelasticity effects. With regard to the numerical results, the effect of the viscous part in the hyperelastic deformation could not be neglected specially in impact loading.

5. Conclusions

Dynamic analysis of the elastomer bushing under different dynamic and impact loadings considered to investigate the mechanical response of the bushing depending on which constitutive law was used. In the first step, three pure hyperelastic models were established for the material in interest. On the basis of uniaxial tensile tests performed at the low rate the hyperelastic constants of the Neo-Hookean, the Mooney-Rivlin and the 3rd order Ogden models were determined. This was done using the Levenberg-Marquardt algorithm for minimizing the distance between the measured point data and the theoretical one. It seems that the Ogden model a better simulates the hyperelastic behavior than the other models. Based on this fact, the Ogden material model used to assess the coupling effects for combined visco and hyperelastic deformations. The quasi-linear theory of viscoelasticity based on Prony series was utilized to develop visco-hyperelastic constitutive equation, in the next step. While in the past there haven't been much research devoted on this specific material because of their complexity, here by superposition of both visco and hyperelastic behaviour we introduced a different method for better describing of these materials. The relaxation time as well as characteristic constants was determined on the basis of the experimental test data by means of an efficient optimization algorithm determining the model that best predicts visco-hyperelastic material behaviour. Implementing the martial models in explicit finite element software, the results of both models designed in LS-DYNA have been compared. Finally these two models subjected to different impact loadings, one axial second transversal, to define which one is the most destructive. According to the obtained results, although hyperelastic models describe elastomers' behaviour but by considering time dependency in these materials, it could be seen that developed visco-hyperelastic model describes these materials more accurately. On the other hand deformation and induced stresses differ considerably by changing the loading rate. It can be concluded that considering viscos effects and time dependency by using visco-hyperelastic model leads us to more accurate results. Comparing two types of impact loading indicates that the transversal loading is more destructive.

References

- Adkins, J.E. and, A.N. (1954), "Gent load-deflexion relations of rubber bush mountings", *Brit. J. Appl. Phys.*, **5**, 340-354.
- Amin, A.F., Alam, M.S. and Okui, Y. (2002), "An improved hyperelasticity relation in modeling viscoelasticity response of natural and high damping rubbers in compression: experiments, parameter identification and numerical verification", *Mech. Mater.*, **34**, 75-95.
- Aniskevich, K., Starkova, O., Jansons, J. and Aniskevich, A. (2010), "Viscoelastic properties of a silica-filled styrene-butadiene rubber under uniaxial tension", *Mech. Compos. Mater.*, **46**, 375-386.
- Bechir, H., Chevalier, L., Chaouche, M. and Boufala, K. (2006), "Hyperelastic constitutive model for rubber-like materials based on the first Seth strain measures invariant", *Eur. J. Mech. A/Solid.*, **25**, 110-

- 124.
- Bergström, J.S. and Boyce, M.C. (1998), "Constitutive modeling of the large strain time-dependent behavior of elastomers", *J. Mech. Phys. Solid.*, **46**, 931-954.
- Björnsson, P. and Danielsson, H. (2005), "Strength and creep analysis of glued rubber foil timber joints", **1**, 145-158.
- Busfield, J.C. and Davies, C.K.L. (2001), "Stiffness of simple bonded elastomer bushes, Part 1-Initial behavior", *Plast. Rub. Compos.*, **30**, 243-257.
- Centeno, O. (2009), *Finite element modeling of a rubber bushing for crash simulation experimental tests and validation*, Structural Mechanics Journal, Sweden.
- Chen, J.S. and Wu, C.T. (1997), "On computational issues in large deformation analysis of rubber bushings", *Mech. Struct. Mach.*, **33**(5), 327-349.
- Diani, J., Brieu, M. and Gilormini, P. (2006), "Observation and modeling of the anisotropic visco-hyperelastic behavior of a rubberlike material", *Int. J. Solid. Struct.*, **43**(10), 3044-3056.
- Fung, Y.C. (1965), *Foundations of solid mechanics*, Upper Saddle River, New Jersey, USA.
- Gavin, H. (2011). "The Levenberg-Marquardt method for nonlinear least squares curve-fitting problems", Department of Civil and Environmental Engineering, Duke University, 1-15.
- Gent, A. (1996), "A new constitutive relation for rubber", *Rub. Chem. Technol.*, **69**, 59-61.
- Goh, S.M., Charalambides, M.N. and Williams, J.G. (2004), "Determination of the constitutive constants of non-linear viscoelastic materials", *Mech. Time-Depend. Mater.*, **8**, 255-268.
- Hakansson, P. (2000), "Finite element modeling of a rubber block exposed to shock loading", Diss. Master's Dissertation, Lund University, Lund, Sweden.
- Hallquist, J.O. (2006), *LS-DYNA Theory Manual*, Livermore Software Technology Corporation.
- Holzappel, G. (1996), "On large strain viscoelasticity: continuum formulation and finite element applications to elastomeric structures", *Int. J. Numer. Meth. Eng.*, **39**, 3903-3926.
- Hopkinton, Simple Bushings_VAD-Lit: www.barrycontrols.com
- Horton, J.M., Gover, M.J. and Tupholme, G.E. (2000), "Stiffness of rubber bush mountings subjected to radial loading", *Rub. Chem. Technol.*, **73**, 253-264.
- Huber, N. and Tsakmakis, Ch. (2000), "Finite deformation viscoelasticity laws", *Mech. Mater.*, **32**, 1-18
- James, J.H. and Guth, E. (1943), "Theory of the elastic properties of rubber", *J. Chem. Phys.*, **11**, 455-481.
- Kadlowec, J., Gerrard, D. and Pearlman, H. (2009), "Coupled axial-torsional behavior of cylindrical elastomer bushings", *Polym. Test.*, **28**, 139-144.
- Kadlowec, J., Wineman, A. and Hulbert, G. (2001), "Coupled response model for elastomeric bushing", *Rub. Chem. Technol.*, **74**(2), 338-352.
- Kadlowec, J., Wineman, A. and Hulbert, G. (2003), "Elastomer bushing response: experiments and finite element modelling", *Acta Mechanica*, **163**, 25-38.
- Khajehsaeid, H., Baghani, M. and Naghdabadi, R. (2013), "Finite strain numerical analysis of elastomeric bushings under multi-axial loadings: a compressible visco-hyperelastic approach", *Int. J. Mech. Mater. Des.*, **9**, 385-399.
- Kim, J., Lee, S. and Min, K.W. (2014), "Design of MR dampers to prevent progressive collapse of moment frames", *Struct. Eng. Mech.*, **52**(2), 291-306.
- Macosko, C.W. and Larson, R.G. (1994), "Rheology: principles, measurements, and applications", **1**, 145-158.
- Martinez, J.M.M. (2006), "Natural rubber by a rubber man", *Mater. Today*, **9**(3), 55-68.
- MATLAB Release (2012b), The MathWorks, Inc., Natick, Massachusetts, United States.
- Moré, J. (1978), *The Levenberg-Marquardt algorithm: implementation and theory*, Numerical analysis, Springer, Berlin Heidelberg.
- Naghdabadi, R., Baghani, M. and Arghavani, J. (2012), "A viscoelastic constitutive model for compressible polymers based on logarithmic strain and its finite element implementation", *Finite Elem. Anal. Des.*, **62**, 18-27.
- Nilesh, D. and Adivi, K.P. (2011), *Modelling of Engine Suspension Components for Crash Simulations*.
- Ogden, R.W. (1972), "Large deformation isotropic elasticity-on the correlation of theory and experiment for

- incompressible rubberlike solids”, *Proceedings of the Royal Society of London A: Mathematical, Physical and Engineering Sciences.*, **326**(67), The Royal Society.
- Okwu, U.N. and Okieimen, F.E. (2011), “Preparation and properties of thioglycollic acid modified epoxidised natural rubber and its blends with natural rubber”, *Eur. Polym. J.*, **37**, 2253-2258.
- Ouyang, X. (2006), “Constitutive equations of rubber under large tensile strain and high strain rates”, Diss. The University of Akron.
- Rivlin, R.S., Barenblatt, G.I. and Joseph, D.D. (1997), *Collected papers of RS Rivlin*, Springer Science & Business Media.
- Suarez, L.E. and Gaviria, C.A. (2015), “Dynamic properties of a building with viscous dampers in non-proportional arrangement”, *Struct. Eng. Mech.*, **55**(6), 1241-1260.
- Treloar, L.R. (2005), *The Physics of Rubber Elasticity*, Oxford University Press, New York.
- Yang, L.M. and Shim, V.P. (2004), “A visco-hyperelastic constitutive description of elastomeric foam”, *Int. J. Impact Eng.*, **30**, 1099-1110.
- Yang, L.M., Shim, V.P.W. and Lim, C.T. (2002), “A visco-hyperelastic approach to modelling the constitutive behaviour of rubber”, *Int. J. Impact Eng.*, **24**, 545-560.
- Yeoh, O.H. and Fleming, P.D. (1997), “A new attempt to reconcile the statistical and phenomenological theories of rubber elasticity”, *J. Polym. Sci. B Polym. Phys. Edit.*, **35**, 1919-1932.